Craniofacial divergence and ongoing adaptation via the hedgehog pathway

Reade B. Roberts[a], Yinan Hu[b], R. Craig Albertson[b,c], and Thomas D. Kocher[a,1]

[a]Department of Biology, University of Maryland, College Park, MD 20742; [b]Department of Biology, Syracuse University, Syracuse, NY 13244; and [c]Department of Biology, University of Massachusetts Amherst, Amherst, MA 01003

Edited by Clifford J. Tabin, Harvard Medical School, Boston, MA, and approved June 27, 2011 (received for review December 8, 2010)

Adaptive variation in craniofacial structure contributes to resource specialization and speciation, but the genetic loci that underlie craniofacial adaptation remain unknown. Here we show that alleles of the hedgehog pathway receptor *Patched1* (*Ptch1*) gene are responsible for adaptive variation in the shape of the lower jaw both within and among genera of Lake Malawi cichlid fish. The evolutionarily derived allele of *Ptch1* reduces the length of the retroarticular (RA) process of the lower jaw, a change predicted to increase speed of jaw rotation for improved suction-feeding. The alternate allele is associated with a longer RA and a more robustly mineralized jaw, typical of species that use a biting mode of feeding. Genera with the most divergent feeding morphologies are nearly fixed for different *Ptch1* alleles, whereas species with intermediate morphologies still segregate variation at *Ptch1*. Thus, the same alleles that help to define macroevolutionary divergence among genera also contribute to microevolutionary fine-tuning of adaptive traits within some species. Variability of craniofacial morphology mediated by *Ptch1* polymorphism has likely contributed to niche partitioning and ecological speciation of these fishes.

adaptive radiation | development | genetics | quantitative trait loci | trophic morphology

The astounding diversity of vertebrate craniofacial morphology reflects adaptation to a wide variety of resources and environments. Evolution of craniofacial structure has been key to niche specialization and speciation in vertebrates (1), most famously exemplified by the varied beak morphology of Darwin's finches (2). The radiation of finches demonstrates both species-defining craniofacial divergence (2) and rapid adaptation of craniofacial morphology within species over the course of a few years in response to changes in resource availability (3). Although shifts in the expression of key craniofacial genes have been correlated with differences in trophic morphology among species of birds and cichlid fishes (4–8), the specific genetic loci producing these differences remain uncharacterized. As a result, it is not clear whether interspecific divergence and intraspecific adaptation share the same molecular genetic basis.

Diversification of trophic morphology in the adaptive radiation of cichlids in Lake Malawi (East Africa) is also correlated with specialized modes of feeding and resource partitioning and has likely contributed to their rapid speciation (9, 10). Because craniofacial structure arises from a complex and dynamic developmental program with both pleiotropic and modular effects (11), the expectation is that it should evolve via continuous fine-tuning steps. In accordance with this prediction, we previously demonstrated that morphological differences between closely related cichlid genera are the result of directional selection on numerous genetic loci of small to moderate effect (8, 12). These studies identified numerous quantitative trait loci (QTL) for craniofacial morphology segregrating in the F_2 hybrid progeny of the genera *Labeotropheus* and *Metriaclima* (8, 12). Although *Labeotropheus* and *Metriaclima* are closely related rock-dwelling cichlid genera, they are divergent in craniofacial morphology and microhabitat utilization (10, 13). *Labeotropheus* is a specialist algal scraper with robust jaws adapted for biting, whereas *Metriaclima* is a generalist with gracile jaws better adapted for suction feeding (Fig. 1 *A* and *B*). These two genera represent opposite ends of the benthic/limnetic ecomorphological continuum that characterizes East African cichlid radiations (10) as well as many other notable divergences among teleosts at both the population and species level (14–19). Identifying the molecular genetic basis for these ecomorphologic shifts therefore has the potential to inform a more comprehensive understanding of teleost diversity in general.

A recent genome scan study identified single nucleotide polymorphisms (SNPs) exhibiting unusually high differentiation (F_{ST}) between *Labeotropheus* and *Metriaclima* (20). The high F_{ST} of these SNPs suggests they may be linked to genetic loci associated with evolutionary divergence between the two genera. Here we compared the genomic locations of the high F_{ST} SNPs and previously identified QTL (8, 12) as a starting point to identify the specific genes contributing to morphological divergence between the genera. We pinpoint alleles of the *Ptch1* gene as contributing to morphological divergence between the two genera and further show that the same alleles of *Ptch1* segregate within other species, producing continuing adaptive effects on craniofacial structure.

Results and Discussion

In a genome scan comparison of *Labeotropheus* and *Metriaclima* (20), SNP Aln100281_1741 had an F_{ST} of 0.86 between the two genera, and a comparative BLAST search placed the SNP in the first intron of the *Ptch1* homolog. We identified a sequence scaffold containing Aln100281 and *Ptch1* from the draft genome assembly of another cichlid fish, the Nile tilapia (*Oreochromis niloticus*). With additional comparative genomics we placed this scaffold on linkage group (LG) 12 of the cichlid genetic map, within a previously identified QTL interval associated with 8.6% of variance in length of the retroarticular process (RA) (8). This QTL was one of five identified for RA length (8). Functionally the inlever for the action of lower jaw depression (Fig. 1*C*), RA length modulates the functional tradeoff between force and velocity during jaw rotation (21, 22). No association was found between the LG12 QTL and outlever length of the lower jaw (8). Shortening of the RA while outlever length remains uniform is predicted to increase the speed of jaw opening, and the LG12 QTL also explains 11.3% of the functional phenotype, the mechanical advantage of jaw opening (MA_O; Fig. 1*C*). We refer to the *Labeotropheus* genotype at the LG12 locus as the "long"-RA allele, and that of *Metriaclima* as the "short"-RA allele, to reflect

Author contributions: R.B.R., R.C.A., and T.D.K. designed research; R.B.R., Y.H., and R.C.A. performed research; R.B.R., Y.H., R.C.A., and T.D.K. analyzed data; and R.B.R., R.C.A., and T.D.K. wrote the paper.

The authors declare no conflict of interest.

This article is a PNAS Direct Submission.

Data deposition: The sequences reported in this paper have been deposited in the GenBank database (accession nos. JN037665–JN037693 and JN116727).

[1]To whom correspondence should be addressed: E-mail: tdk@umd.edu.

This article contains supporting information online at www.pnas.org/lookup/suppl/doi:10.1073/pnas.1018456108/-/DCSupplemental.

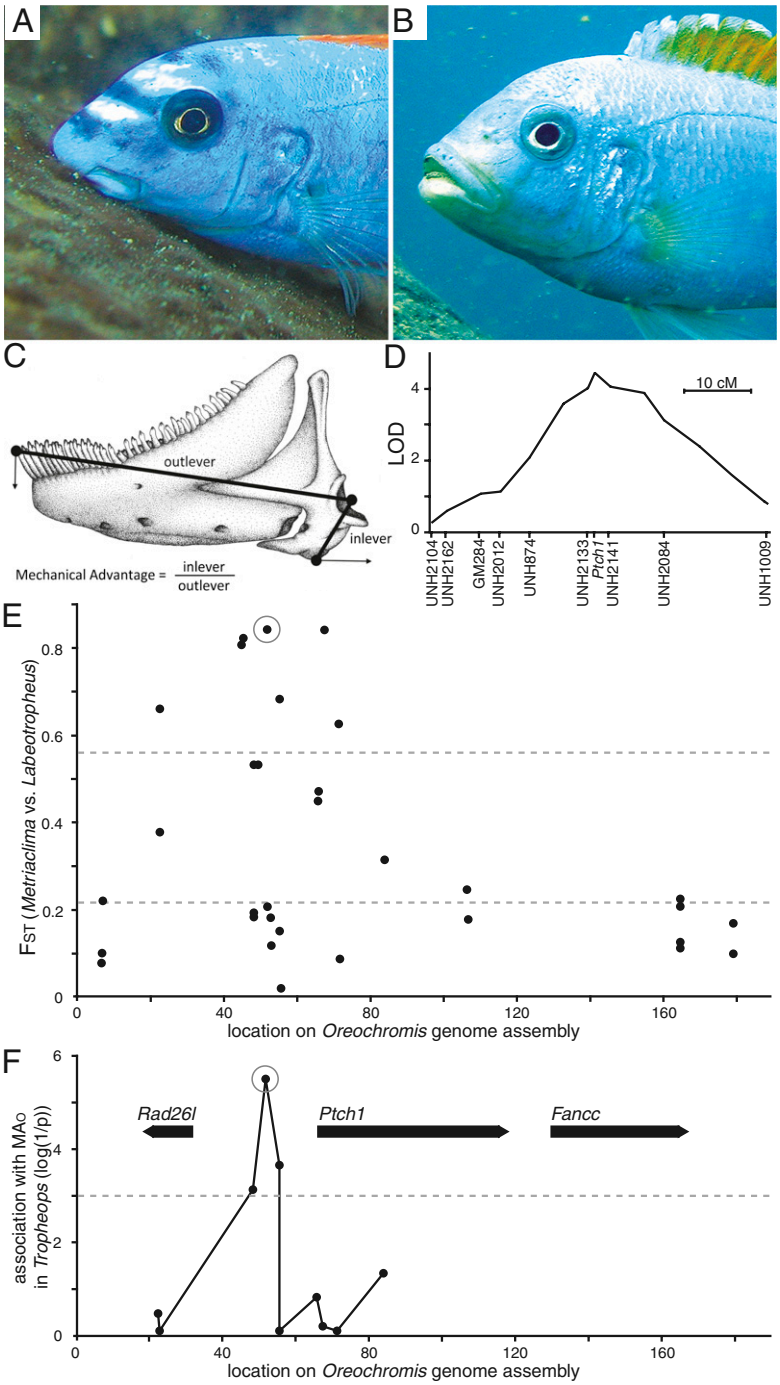

Fig. 1. *Ptch1* locus characterization in families, genera, and populations. Craniofacial appearance of (*A*) *Labeotropheus trewavasae* (image courtesy of Justin Marshall) and (*B*) *Metriaclima mbenjii*. (*C*) Lower jaw phenotype measures; RA and inlever length is equivalent. (*D*) QTL mapping interval for MA_O on cichlid LG12. (*E*) Population differentiation (F_{ST}) between *Labeotropheus* and *Metriaclima* (n = 24 each) for SNPs at the *Ptch1* locus. Dashed lines indicate two experimental measures of mean F_{ST}; the lower line from global comparison of *Labeotropheus* vs. *Metriaclima* across many populations (20), and the upper line from comparisons of randomized *Labeotropheus* and *Metriaclima* population pairs from distinct sites (48). (*F*) Significance of association between SNPs at the *Ptch1* locus and MA_O in the genus *Tropheops* (Wald test, n = 59); dashed line indicates a P value of 0.001. Genes in the region annotated with bold arrows. The SNP used to indicate long and short alleles of *Ptch1* is circled in *E* and *F*.

the morphological phenotypes associated with each. The long allele acts dominantly to increase RA length and MA_O (8).

Population Genetic Mapping of the Causative Interval. We developed additional markers across the *Ptch1* genome scaffold by resequencing a panel of Malawi cichlid DNA to identify polymorphisms (Table S1). Genotyping the F_2 mapping family for a marker adjacent to *Ptch1* confirmed its location on LG12 and centers the QTL interval squarely over this locus (Fig. 1*D*). We then used a DNA panel consisting of four *Labeotropheus* and four *Metriaclima* wild-caught populations to characterize patterns of sequence divergence in the region (Table S2). The SNP Aln100281_1741 continued to show high F_{ST} between genera in the populations included in the panel. Several markers located as

far as 20 kb upstream of *Ptch1* also exhibited extremely high F_{ST}, approaching alternate fixation (Fig. 1*E*). The consistency of genetic divergence between *Labeotropheus* and *Metriaclima* across species and populations suggests that variation in this region underlies a fundamental phenotypic difference between the two genera.

Although genetic differentiation at *Ptch1* is coincident with the QTL for RA length, the *Labeotropheus* and *Metriaclima* panel does not allow correlation of genotype to a specific phenotype within populations because alternate alleles are essentially fixed within each genus. However, these alleles are segregating within populations of a third genus, *Tropheops*, which exhibits a range of trophic morphology roughly intermediate between *Metriaclima* and *Labeotropheus* (23, 24). Thus, we were able to directly measure association between individual MA_O phenotypes and markers across the high F_{ST} region, using a panel of four natural populations of *Tropheops* (Table S2). The association peaks at an SNP roughly 15 kb upstream of *Ptch1* and falls below significance before the *Ptch1* start codon (Fig. 1*F*). The genotype–phenotype association within and among *Tropheops* species provides strong evidence that the *Ptch1* locus is modulating RA length and MA_O and narrows the interval of interest to the region upstream of the gene (Figs. 1*F* and 2). The upstream SNPs serve to label long and short alleles at the locus; as in the F_2 mapping family, the long allele seems to be dominant over the short allele in natural *Tropheops* populations (Fig. 2).

***Ptch1* Expression Differences Correlate with Developmental Divergence.** We did not find any nonsynonymous polymorphisms in *Ptch1* coding sequence. The lack of structural differences in the protein is not surprising given the fundamental importance of *Ptch1* to a variety of developmental processes (25). Because signatures of genetic divergence immediately upstream of *Ptch1* suggest adaptation via *cis*-regulatory elements, we examined *Ptch1* expression by in situ hybridization. Dimensionality of the lower jaw is determined early, and in comparisons of *Labeotropheus* and *Metriaclima* differences in the shape of the lower jaw precursor (Meckel's cartilage) are evident as early as 5 d postfertilization (dpf), stage 10 (8, 26). By the following day (stage 12) many of the bones that constitute the feeding apparatus have begun to condense, and at this early stage we observed discrete nodes of *Ptch1* expression in areas where bone development has or will be initiated (Fig. 3 *B–D* and *F–H*). Notably, species exhibit differences in *Ptch1* expression that correlate with biting and suction feeding jaw morphologies. In the long RA species *Labeotropheus fuelleborni* (LF) there is marked expression of *Ptch1* surrounding the lower jaw at this stage, with nodes of robust expression in or adjacent to areas of skeletal differentiation, including the regions where the dentary and RA will form (Fig. 3 *B* and *D*). In contrast, levels of *Ptch1* are much lower in the short RA species *Metriaclima zebra* (MZ) in the same context (Fig. 3 *F* and *H*). Unlike expression at the developing lower jaw, levels of *Ptch1* expression are qualitatively similar between LF and MZ in the developing fin-ray elements of the tail (Fig. 3 *C* and *G*).

To more accurately describe regional differences in levels of expression of *Ptch1*, as well as its downstream target *Gli1*, we performed a pixel density analysis on stage-matched LF and MZ larvae as previously described (27, 28). We find that a significantly greater proportion of pixels were labeled in the jaws of LF compared with MZ for both *Ptch1* and *Gli1* (Fig. S1 and Table S3). No difference was observed for either factor in the caudal fin (Fig. S1 and Table S3). Additionally, a quantitative PCR assay for *Ptch1* transcript in microdissected tissues from 6.5-dpf larvae demonstrated higher levels of *Ptch1* transcript in the lower jaw of LF relative to MZ, but there was no difference in *Ptch1* transcript levels in the trunk and tail by species (Table S4). Together these data strongly support the assertion that PTCH1-mediated hedgehog signaling is up-regulated in the jaws of LF compared with MZ, specifically at the time and within the area where the RA develops.

Manipulation of Hedgehog Pathway Signaling Affects Bone Development and Recapitulates Natural Interspecific Variation in Bone Shape. Our expression results are consistent with recent work demonstrating a role for hedgehog signaling in dermal bone development (29, 30) and predict that modulation of this pathway can lead to variation in jaw shape. To test this prediction we treated LF larvae with cyclopamine, an antagonist of hedgehog pathway signaling (31), at a critical stage of craniofacial bone development and *Ptch1* expression (stage 12). During normal development, both *Ptch1* and its downstream target *Gli1* are expressed in areas adjacent to or coincident with the bone differentiation marker *Col1a1* (Fig. S1 *A–L*). In treated larvae, we

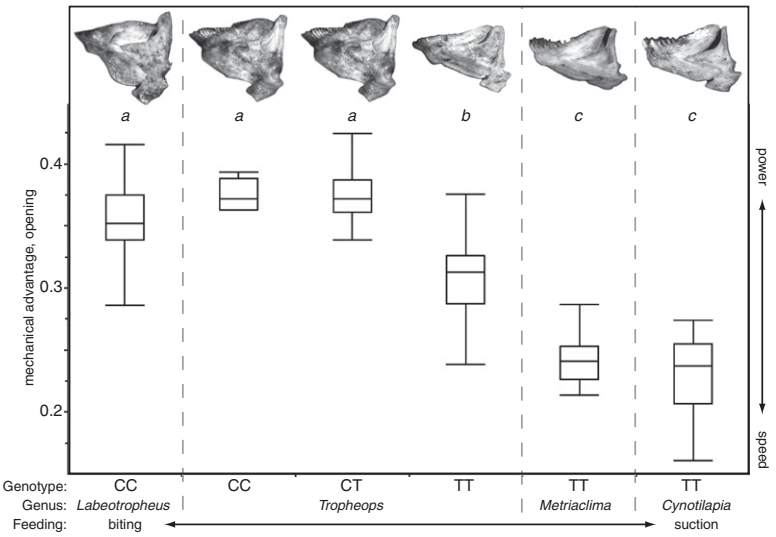

Fig. 2. Morphology and function of the lower jaw by genus and *Ptch1* genotype. MA_O values of wild individuals (Table S2) indicated by box-plot, with letters above designating statistical groups by one-way ANOVA and Tukey's honest significance test ($P < 0.05$). Lower jaw images from representative individuals at top; each jaw has an MA_O matching the mean of the corresponding genus and genotype. Genotype refers to high-association SNP (circled in Fig. 1 *E* and *F*). Box boundaries indicate quartiles, and whiskers indicate range of MA_O data.

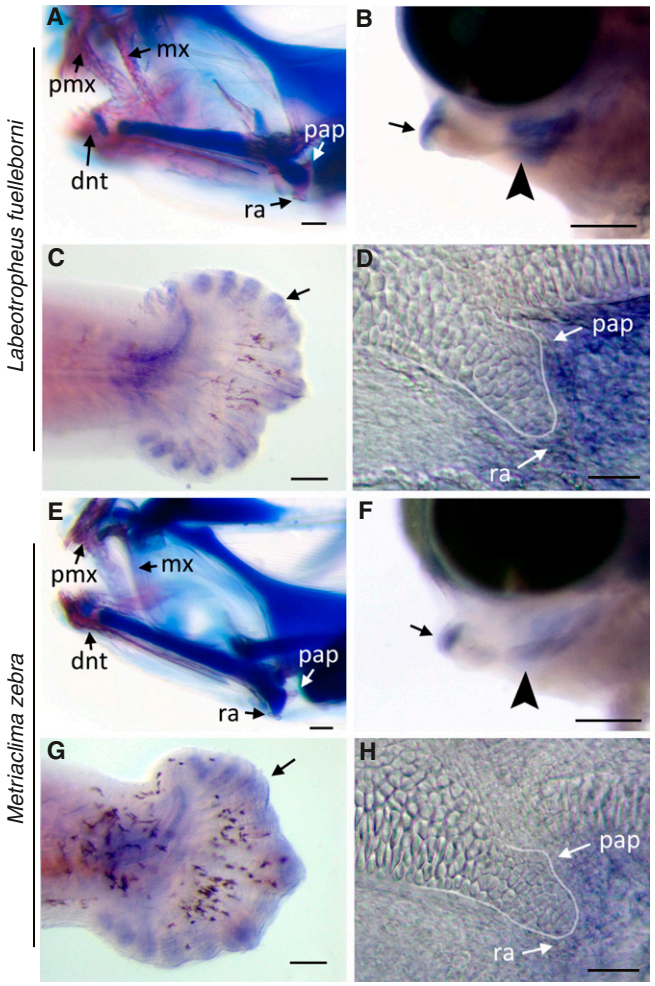

Fig. 3. Interspecific differences in *Ptch1* expression during cichlid craniofacial development. Craniofacial outcomes in (*A*) LF and (*E*) MZ larvae at 13 dpf; LF larvae exhibit accelerated bone (pink) development compared with MZ; cartilage stains blue. *Ptch1* in situ labeling in representative 6-dpf (stage 12) (*B–D*) LF and (*F–H*) MZ larvae: (*B* and *F*) Lateral whole-mount view of lower jaw with nodes of *Ptch1* expression, particularly in mesenchymal cells at the distal (arrow) and proximal (arrowhead) ends of the lower jaw precursor where the dentary and RA process will form, respectively. (*C* and *G*) *Ptch1* labeling is qualitatively similar in developing fin-ray elements of tail (arrows). (*D* and *H*) Flat-mount preparation of the jaw joint in lateral view, showing the cartilaginous precursor of the RA process (outlined) relative to node of *Ptch1* expression. dnt, dentary; mx, maxilla; pap, posterior articulation process; pmx, premaxilla. (Scale bars, 200 μm in *A, B, E,* and *F*; 100 μm in *C* and *G*; and 10 μm in *D* and *H*.)

find that expression of both *Ptch1* and *Gli1* is dramatically and globally reduced (Fig. S1 *P–W* and Table S3). We also find that bone development is delayed in areas where *Ptch1* is normally expressed (Fig. S1 *X–AA* and Table S3). Specifically, less *Col1a1* expression was observed around the developing RA, whereas more cells were expressing *Col1a1* around the branchiostegal rays and within the caudal fin (Fig. S1 *Y–AA* and Table S3), suggesting that these structures were in a more undifferentiated state after cyclopamine treatment relative to control animals. Expression of *Col1a1* around the dentary was relatively unaffected by cyclopamine treatment (Fig. S1*X*); however, this is likely because development of this structure was well underway at the stage when animals were treated. Overall, these patterns of expression are consistent with the phenotypic outcome of cyclopamine treatment. Specifically, we find that cyclopamine-treated larvae exhibit significantly reduced RA length (and MA_O), whereas the dentary and overall length of the lower jaw, which is determined primarily by outgrowth of Meckel's cartilage that occurs earlier than the stages examined here, remains roughly the same (Fig. 4 *A–C* and Table S5). In terms of gene expression patterns (Fig. S1 and Table S3), relative bone development (Fig. S1 and Table S3), and MA_O (Fig. 4 *A–C* and Table S5), cyclopamine-treated LF recapitulate a suction-feeding, MZ-like lower jaw phenotype. Although rates of overall development do not differ between LF and MZ during early larval stages, we suggest that key differences in lower jaw shape are due at least in part to PTCH1-mediated differences in the rate of bone development within the RA. The exact cellular mechanism(s) through which hedgehog signaling influences differences in bone development remain to be characterized.

We also noted that treated animals exhibited bifurcated expression of *Col1a1* within the developing branchiostegal rays (asterisk in Fig. S1*Z*), as well as aberrant expression within the dermal fin ray elements of the caudal fin (arrow in Fig. S1*AA*). These patterns are also consistent with craniofacial defects after cyclopamine treatment, in which fusion of the branchiostegal rays and truncation of the caudal fin ray elements were observed. These data extend previously documented roles for hedgehog signaling in dermal bone development (29, 30) and suggest that this pathway plays an important role in polarizing dermal bone development along a proximal–distal axis. It is well established that hedgehog signaling is critical for the proper patterning and polarization of several organs in various animal taxa (32–37), but here a similar role has been documented for bone development. The extent to which hedgehog-mediated outgrowth of other dermal bones (e.g., RA) has influenced species-specific differences in craniofacial shape would be a fruitful area of future investigation.

Our data suggest the presence of at least two functionally distinct alleles of *Ptch1* that produce different levels of transcript in a spatially and temporally restricted manner. The long allele produces relatively higher levels of *Ptch1*, resulting in greater bone deposition, a longer RA, and higher MA_O. The short allele has relatively lower expression, resulting in less bone and a shorter RA that increases jaw opening speed. Although the association between *Ptch1* expression and bone deposition is interesting, we find no significant association between *Ptch1* genotype and length or thickness of the jaw, suggesting that differences in developmental outcomes of the *Ptch1* alleles are largely restricted to the RA. Whether the early effects of Ptch1-mediated bone deposition represent an adaptation for the timing and/or rate of bone development among cichlids remains an open question. Certainly the results of our expression and cyclopamine experiments support a role for hedgehog signaling in modulating bone development.

***Ptch1* Alleles Contribute to Microevolutionary and Macroevolutionary Processes.** Using the SNP in highest association with MA_O in *Tropheops*, we genotyped the *Ptch1* locus in additional wild-caught individuals of four genera (Fig. 2). The significant correlation to MA_O phenotype remains consistent across all taxa measured, suggesting extremely tight linkage of the SNP with the causative polymorphism. Obligate biters (*Labeotropheus)* and suction feeders (*Cynotilapia* and *Metriaclima*) are nearly fixed for long and short alleles, respectively. The genus *Tropheops* is particularly interesting, because segregating *Ptch1* alleles contribute to "shallow" and "deep" ecomorphs that correlate with resource use and depth distribution (24, 38). In deep ecomorph *Tropheops* species, the short *Ptch1* allele seems to be fixed, contributing to a morphology adapted to sifting and suction feeding of loose material. In the *Tropheops* populations examined from shallow water, the two alleles segregate and are associated with different morphologies within species. Individuals carrying a long allele at *Ptch1* have a jaw morphology similar to that of *Labeotropheus*, well adapted for

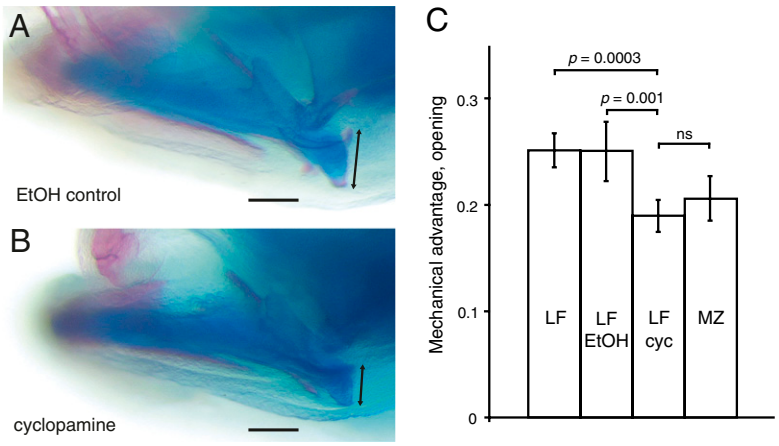

Fig. 4. Treatment of biting species larvae with a hedgehog pathway inhibitor recapitulates a suction-feeding jaw phenotype. LF larvae were treated with (*A*) 0.5% ethanol (EtOH control, $n = 7$) or (*B*) 50 μM cyclopamine (cyc, $n = 10$) for 6 h at stage 12; RA length measured at 12 dpf (black arrow in *A* and *B*). (*C*) Relative to the length of the lower jaw (measured as the distance between the center of the jaw joint and the tip of the dentary), RA length (measured as the distance from the posterior tip of the posterior articulation process to the ventral tip of the retroarticular) was significantly reduced in cyclopamine treatment group compared with the control LF group but was not significantly different from MZ control larvae ($n = 7$). Larvae treated with ethanol were indistinguishable from untreated siblings ($n = 6$). *P* values, one-way ANOVA. (Scale bar, 100 μm.)

feeding on attached algae found at shallow depth in the lake. Individuals homozygous for the short allele of *Ptch1* have a trophic morphology that more closely resembles that of the deep ecomorphs, better suited for sifting and suction feeding on loose material. Thus, allelic variation at the *Ptch1* locus is associated with the continuum in lower jaw morphology both within and among *Tropheops* species. Although these data are consistent with recent work showing that early Sonic hedgehog signaling from the embryonic forebrain can lead to continuous craniofacial variation in mouse embryos (39) and jaw width differences in the Mexican tetra (40), our results posit a unique role for hedgehog signaling in regulating fine-scale, continuous differences in feeding morphology via bone deposition.

Overtly, the genus *Labeotropheus* has a highly specialized trophic apparatus, whereas the genus *Metriaclima* has a generalist morphology, more similar to that of the ancestral lineages that invaded Lake Malawi (10). It is therefore surprising that, according to a *Ptch1* gene phylogeny including other African cichlid genera from Lake Malawi and beyond (Fig. S2), the short *Ptch1* allele fixed in *Metriaclima* is more recently derived, whereas *Labeotropheus* carries the ancestral allele. The SNP haplotype that labels the short allele is found in only a subset of the rock-dwelling cichlids in Malawi. The short allele also shows signatures of recent selection, including relatively higher extended haplotype homozygosity, reduced nucleotide diversity, and significantly low values for Tajima's *D* (Fig. S3). These data suggest that selection has acted recently to fine-tune the RA to improve suction feeding within the rock-dwelling cichlids.

East African rift-valley cichlid radiations are characterized by rapid and repeated bentho-pelagic divergence following the colonization of a lacustrine environment by riverine ancestors (10). In Lake Malawi this divergence has led to the establishment of the genetically distinct rock- and sand-dwelling clades (41, 42). On average, rock-dwelling species possess trophic morphologies consistent with a benthic lifestyle, whereas most sand-dwellers are pelagic in terms of their feeding ecology (10). We propose that, after an initial colonization of the rock niche by cichlids with specialized biting morphologies, selection for the short allele of *Ptch1* contributed to the reevolution of an ancestral-like feeding strategy and concomitant expansion of the rock-dwelling niche into the water column.

Despite the major and conserved roles the hedgehog pathway plays throughout development, we show that it continues to evolve to produce adaptive changes in craniofacial phenotype. Notably, we demonstrate that the same *Ptch1* alleles underlying macroevolutionary divergence between genera also form the basis of microevolutionary adaptation among species and even within populations. Where *Ptch1* alleles segregate, a range of ecologically relevant morphologies are produced within populations. Importantly, the resources used by segregating ecomorphs are distributed by depth, providing an opportunity for spatial segregation of individuals by genotype within populations, possibly contributing to character displacement and even the development of incipient species (43). Thus, diversification via adaptive polymorphism could support iterative niche partitioning in complex communities. Additionally, such adaptive polymorphism segregating within populations would permit rapid morphological evolution to take place in response to sudden environmental change. Segregating fine-tuning alleles of the kind we describe here have likely been a key component in both adaptation and speciation in the ongoing explosive radiation of Lake Malawi cichlids.

Materials and Methods

Animals. Fish for breeding and association studies were collected directly from Lake Malawi. Fish were maintained and euthanized according to Institutional Animal Care and Use Committee guidelines. Larval fish were obtained by natural matings within facilities at Syracuse University and the University of Maryland, with developmental staging based on de Jong et al. (26). A hybrid cross between LF and MZ generated an F2 mapping population ($n = 173$), which was phenotyped for jaw morphology and used as the basis of QTL analysis as previously described (8, 12).

Genetic Analysis. Draft sequence of the *O. niloticus* genome was assembled from Illumina sequence reads totaling 60× sequence coverage. The assembly has an N50 scaffold size of 138 kb and was aligned to stickleback genome sequence using BLAST (available at http://BouillaBase.org). Shotgun genome sequence of Malawi cichlid species (20) was aligned to the *Oreochromis* genome assembly using BLASTN. Other polymorphisms were identified (Table S1) and genotyped by resequencing aligned sequences using Applied Biosystems Big Dye Terminator chemistry and an ABI3730 sequencer. The marker Ptch1Loc10_SNP1 was added to the genetic map as "*Ptch1*" by genotyping the original F2 mapping family (12); the resulting map was used for QTL analysis. Population genetic and association analyses were performed in DnaSP and PLINK, respectively (44, 45), using polymorphisms with a minor allele frequency >0.05.

In Situ Hybridization. Whole-mount in situ hybridization (WISH) was performed as previously described (8). Embryos used for the reported experi-

ments were raised, staged, fixed, and processed in parallel. Sense and antisense *Ptch1* riboprobes were made from cichlid clones (sequence identical for LF, accession no. JN037690, and MZ, accession no. JN037691), corresponding to exons 1–7 and 7–17. These yielded identical WISH results; data derived from the exons 1–7 riboprobe are reported. Accession numbers for *Gli1* and *Col1a1* probes are JN037689 and JN116727, respectively. To facilitate probe penetration, alkaline hydrolysis was used to fragment probes to ≈500 bp. A solution of 20 mL RNA probe, 12 mL H_20, 4 mL 0.4 M sodium bicarbonate, and 4 mL 0.6 M sodium carbonate was incubated at 60 °C for a period based on the following: time (min) = (starting kb − desired kb)/(0.11 × starting kb × desired kb).

Pharmacological Treatment. On the basis of previously published work in cichlids, we used cyclopamine (LC Laboratories) at a working concentration of 50 μM (46). Cyclopamine (10 mM, in ethanol) or ethanol alone (control) was added to larval fish water. Animals were treated for 6 h in the dark because cyclopamine is light sensitive. After treatment, larvae were washed several times in fish water before returning to circulating culture flasks to be grown out to 12 dpf. Cartilage and bone staining was performed as previously described (47). Larvae were photographed with a Zeiss Axiocam digital imaging system mounted to an M2 Bio stereomicroscope (Zeiss). Image processing and pixel density analysis was performed in Adobe Photoshop CS4 (Fig. S4).

ACKNOWLEDGMENTS. We thank Matthew Conte for bioinformatics support; Claire O'Quin and Jennifer Ser for fish husbandry support; Rolf Karlstrom for advice on cyclopamine treatment in fish; Justin Marshall for the *Labeotropheus* photograph used in Fig. 1; and J. Todd Streelman, William Jeffery, Karen Carleton, and Kelly O'Quin for their comments on previous drafts of the manuscript.

1. Gans C, Northcutt RG (1983) Neural crest and the origin of vertebrates: A new head. *Science* 220:268–273.
2. Darwin CR (1845) *Journal of Researches into the Geology and Natural History of the Various Countries Visited During the Voyage of H.M.S. Beagle, Under the Command of Captain FitzRoy, R.N* (John Murray, London), 2nd Ed.
3. Grant PR, Grant BR (2002) Unpredictable evolution in a 30-year study of Darwin's finches. *Science* 296:707–711.
4. Abzhanov A, Protas M, Grant BR, Grant PR, Tabin CJ (2004) Bmp4 and morphological variation of beaks in Darwin's finches. *Science* 305:1462–1465.
5. Abzhanov A, et al. (2006) The calmodulin pathway and evolution of elongated beak morphology in Darwin's finches. *Nature* 442:563–567.
6. Wu P, Jiang TX, Suksaweang S, Widelitz RB, Chuong CM (2004) Molecular shaping of the beak. *Science* 305:1465–1466.
7. Wu P, Jiang TX, Shen JY, Widelitz RB, Chuong CM (2006) Morphoregulation of avian beaks: Comparative mapping of growth zone activities and morphological evolution. *Dev Dyn* 235:1400–1412.
8. Albertson RC, Streelman JT, Kocher TD, Yelick PC (2005) Integration and evolution of the cichlid mandible: the molecular basis of alternate feeding strategies. *Proc Natl Acad Sci USA* 102:16287–16292.
9. Kocher TD (2004) Adaptive evolution and explosive speciation: The cichlid fish model. *Nat Rev Genet* 5:288–298.
10. Cooper WJ, et al. (2010) Bentho-pelagic divergence of cichlid feeding architecture was prodigious and consistent during multiple adaptive radiations within African rift-lakes. *PLoS ONE* 5:e9551.
11. Helms JA, Schneider RA (2003) Cranial skeletal biology. *Nature* 423:326–331.
12. Albertson RC, Streelman JT, Kocher TD (2003) Directional selection has shaped the oral jaws of Lake Malawi cichlid fishes. *Proc Natl Acad Sci USA* 100:5252–5257.
13. Albertson RC, Kocher TD (2001) Assessing morphological differences in an adaptive trait: A landmark-based morphometric approach. *J Exp Zool* 289:385–403.
14. Skulason S, Noakes DLG, Snorrason SS (1989) Ontogeny of trophic morphology in four sympatric morphs of arctic charr *Salvelinus alpinus* in Thingvallavatn, Iceland. *Biol J Linn Soc Lond* 38:281–301.
15. Walker JA (1997) Ecological morphology of lacustrine threespine stickleback *Gasterosteus aculeatus* L. (Gasterosteidae) body shape. *Biol J Linn Soc Lond* 61:3–50.
16. Adams CE, Huntingford FA (2002) The functional significance of inherited differences in feeding morphology in a sympatric polymorphic population of Arctic charr. *Evol Ecol* 16:15–25.
17. Parsons KJ, Robinson BW (2006) Replicated evolution of integrated plastic responses during early adaptive divergence. *Evolution* 60:801–813.
18. Riopel C, Robinson BW, Parsons KJ (2008) Analyzing nested variation in the body form of Lepomid sunfishes. *Environ Biol Fishes* 82:409–420.
19. Cooper WJ, Westneat MW (2009) Form and function of damselfish skulls: Rapid and repeated evolution into a limited number of trophic niches. *BMC Evol Biol* 9:24.
20. Loh YH, et al. (2008) Comparative analysis reveals signatures of differentiation amid genomic polymorphism in Lake Malawi cichlids. *Genome Biol* 9:R113.
21. Liem KF (1978) Modulatory multiplicity in the functional repertoire of the feeding mechanism in cichlid fishes. *J Morphol* 158:323–360.
22. Westneat MW (1990) Feeding mechanics of teleost fishes (Labridae; Perciformes): A test of four-bar linkage models. *J Morphol* 205:269–295.
23. Albertson RC, Kocher TD (2005) Genetic architecture sets limits on transgressive segregation in hybrid cichlid fishes. *Evolution* 59:686–690.
24. Albertson RC (2008) Morphological divergence predicts habitat partitioning in a Lake Malawi cichlid species complex. *Copeia* 2008:689–698.
25. Carroll SB (2005) Evolution at two levels: On genes and form. *PLoS Biol* 3:e245.
26. de Jong IM, Witte F, Richardson MK (2009) Developmental stages until hatching of the Lake Victoria cichlid *Haplochromis piceatus* (Teleostei: Cichlidae). *J Morphol* 270: 519–535.
27. Albertson RC, Yelick PC (2007) Fgf8 haploinsufficiency results in distinct craniofacial defects in adult zebrafish. *Dev Biol* 306:505–515.
28. Cooper WJ, Albertson RC (2008) Quantification and variation in experimental studies of morphogenesis. *Dev Biol* 321:295–302.
29. Abzhanov A, Rodda SJ, McMahon AP, Tabin CJ (2007) Regulation of skeletogenic differentiation in cranial dermal bone. *Development* 134:3133–3144.
30. Hammond CL, Schulte-Merker S (2009) Two populations of endochondral osteoblasts with differential sensitivity to Hedgehog signalling. *Development* 136:3991–4000.
31. Chen JK, Taipale J, Cooper MK, Beachy PA (2002) Inhibition of Hedgehog signaling by direct binding of cyclopamine to Smoothened. *Genes Dev* 16:2743–2748.
32. Chuong CM, Patel N, Lin J, Jung HS, Widelitz RB (2000) Sonic hedgehog signaling pathway in vertebrate epithelial appendage morphogenesis: Perspectives in development and evolution. *Cell Mol Life Sci* 57:1672–1681.
33. Koyama E, et al. (1996) Polarizing activity, Sonic hedgehog, and tooth development in embryonic and postnatal mouse. *Dev Dyn* 206:59–72.
34. Ingham PW, Fietz MJ (1995) Quantitative effects of hedgehog and decapentaplegic activity on the patterning of the *Drosophila* wing. *Curr Biol* 5:432–440.
35. Krauss S, Concordet JP, Ingham PW (1993) A functionally conserved homolog of the *Drosophila* segment polarity gene hh is expressed in tissues with polarizing activity in zebrafish embryos. *Cell* 75:1431–1444.
36. Tanaka M, et al. (2000) Distribution of polarizing activity and potential for limb formation in mouse and chick embryos and possible relationships to polydactyly. *Development* 127:4011–4021.
37. Harris MP, Williamson S, Fallon JF, Meinhardt H, Prum RO (2005) Molecular evidence for an activator-inhibitor mechanism in development of embryonic feather branching. *Proc Natl Acad Sci USA* 102:11734–11739.
38. Ribbink AJ, Marsh BA, March AC, Ribbink AC, Sharp BJ (1983) A preliminary survey of the cichlid fishes of rocky habitats in Lake Malawi. *S Afr J Zool* 18:149–310.
39. Young NM, Chong HJ, Hu D, Hallgrímsson B, Marcucio RS (2010) Quantitative analyses link modulation of sonic hedgehog signaling to continuous variation in facial growth and shape. *Development* 137:3405–3409.
40. Yamamoto Y, Byerly MS, Jackman WR, Jeffery WR (2009) Pleiotropic functions of embryonic sonic hedgehog expression link jaw and taste bud amplification with eye loss during cavefish evolution. *Dev Biol* 330:200–211.
41. Albertson RC, Markert JA, Danley PD, Kocher TD (1999) Phylogeny of a rapidly evolving clade: the cichlid fishes of Lake Malawi, East Africa. *Proc Natl Acad Sci USA* 96:5107–5110.
42. Danley PD, Kocher TD (2001) Speciation in rapidly diverging systems: Lessons from Lake Malawi. *Mol Ecol* 10:1075–1086.
43. Mayr E (1963) *Animal Species and Evolution* (Harvard Univ Press, Cambridge, MA).
44. Librado P, Rozas J (2009) DnaSP v5: A software for comprehensive analysis of DNA polymorphism data. *Bioinformatics* 25:1451–1452.
45. Purcell S, et al. (2007) PLINK: A tool set for whole-genome association and population-based linkage analyses. *Am J Hum Genet* 81:559–575.
46. Fraser GJ, Bloomquist RF, Streelman JT (2008) A periodic pattern generator for dental diversity. *BMC Biol* 6:32.
47. Walker MB, Kimmel CB (2007) A two-color acid-free cartilage and bone stain for zebrafish larvae. *Biotech Histochem* 82:23–28.
48. Mims MC, Darrin Hulsey C, Fitzpatrick BM, Streelman JT (2010) Geography disentangles introgression from ancestral polymorphism in Lake Malawi cichlids. *Mol Ecol* 19:940–951.